M&C 2001 Salt Lake City, Utah, USA, September 2001.

A NODAL INTEGRAL METHOD FOR THE DISSIPATIVE SHALLOW-WATER EQUATIONS WITH CORIOLIS FORCE

Brian E. Mays and J. Dorning
University of Virginia
Charlottesville, VA 22903-2442
bem5r@virginia.edu dorning@virginia.edu

Keywords: Numerical methods, nodal methods, shallow-water equations, computational fluid dynamics

ABSTRACT

A new nodal integral method for the solution of the two-dimensional shallow-water equations with second-order subscale dissipation is developed and applied to several test problems. To develop this method, the partial differential equations are transverse averaged over each space-time computational element, and the resulting ordinary differential equations are solved analytically to yield a set of local integral equations, expressed in terms of the dependent variables averaged along the element interfaces. The remaining parts of the equations, collected in source-like terms prior to the transverse-averaging procedure, are approximated by low-order expansions to complete the discretization process. The result is a set of nonlinear algebraic equations for each time step, which is solved using a Newton-Krylov method.

The new method is applied to several test problems with analytical solutions to establish its accuracy, including simple steady-state flows and fairly complicated time-dependent Rossby wave problems. It also is applied to complex benchmark problems involving flows over obstacles and jet-driven flows.

1. INTRODUCTION

Since its inception, the nodal integral approach has been used to develop methods for the highly accurate numerical solution of fluid flow problems. It was introduced by Azmy and Dorning (1983) in their development of a nodal integral method (NIM)—building on an earlier nodal method (Horak, 1985)—to solve the Navier-Stokes equations for two-dimensional, steady-state fluid flows. Other NIMs for fluid flow problems, based on this approach, followed. Wilson, et al. (1987) used it to develop a method for time-dependent two-dimensional flows, and Decker and Dorning (1993) used it to develop a method for time-dependent three-dimensional flows.

These methods have proven to be highly accurate and efficient, reducing the CPU time required to calculate inlet flow between parallel plates by a factor of fifty, when compared to finite-difference calculations with the same accuracy, and reducing the CPU time required for the modified driven cavity problem by a factor of over a thousand (Azmy, 1983). Other applications of the NIM to fluid flow problems (Azmy, 1984, 1986) have used grids that are far coarser than those required by finite-difference methods to achieve the same accuracy.

Although these methods have achieved great success in solving the Navier-Stokes equations and natural convection problems, little has been done to extend them to more complicated systems of equations, such as those encountered in large-scale atmospheric modeling. We have developed a new NIM for the archetypical equations for such systems: the shallow-water equations.

1.1 The Shallow-Water Equations

The shallow-water equations describe the dynamics of a thin layer of homogeneous, incompressible fluid flowing at low speeds. For atmospheric flows, they are derived via a scaling argument from the full equations of motion governing the fluid: the three-dimensional Navier-Stokes equations with an additional Coriolis term to account for the rotation of the coordinate frame. By arguing that the horizontal scale of the motion is much larger than the vertical scale, the fluid can be assumed to be in hydrostatic equilibrium at all times, and therefore the horizontal pressure gradient throughout the fluid depends only upon the height of the free surface (at the top of the fluid). This eliminates all stratification, and the equations of motion that result can be expressed in terms of the (two-dimensional) horizontal velocity and the height of the free surface. Although these equations describe the motion of a shallow, three-dimensional, incompressible fluid, they also are equivalent to the equations of motion for a two-dimensional, compressible fluid with Coriolis force; hence, the method developed here also applies directly to those equations.

The shallow-water equations can be applied to many flow problems involving shallow fluid layers; however, they are most commonly used to model large-scale atmospheric and oceanic flows, which could include plumes from nuclear power plants or from nuclear weapons tests. They do not represent the complete atmospheric or oceanic system, since they do not include the vertical momentum or the thermodynamic equations. Nevertheless, they provide a useful first step for developing new numerical methods for these systems, since they include all the major difficulties found in the horizontal aspects of three-dimensional atmospheric or oceanic modeling, while avoiding the need to simultaneously treat the complexities of the thermodynamics of a density-stratified fluid.

In their advective form, the shallow-water equations are written

$$\frac{\partial \mathbf{V}}{\partial t} + (\mathbf{V}\cdot\nabla)\,\mathbf{V} + f\,\mathbf{k}\times\mathbf{V} = K\nabla^2\mathbf{V} - \nabla\Phi$$

$$\frac{\partial h}{\partial t} + (\mathbf{V}\cdot\nabla)\,h + h\nabla\cdot\mathbf{V} = 0$$

where $\mathbf{V}$ is the two-dimensional velocity, $\Phi = gh + gh_B$ is the geopotential at the free surface, h is the depth of the fluid, h_B is the height of the rigid bottom, g is gravity, and f is the Coriolis parameter. The specific form of these equations that we consider is for the β-plane model, an approximation to the shallow-water equations on a sphere in which the curved surface is locally approximated by a Cartesian coordinate system and the variation of Coriolis parameter with latitude is approximated by a first-order expansion: $f = f_0 + \beta y$. Unlike the NIM developed for the shallow-water equations by Hannon, et al. (1991), the new method includes a second-order, linear dissipative term. In this term, K is the kinematic viscosity of a viscous fluid, or in the case of atmospheric flows where the scale of motion is sufficiently large that the molecular viscosity becomes insignificant, it represents a "turbulent viscosity," one way of modeling the loss of energy from the large-scale motion through the action of subscale turbulence.

2. FORMULATION OF THE METHOD

The nodal integral approach is the procedure through which a partial differential equation is transverse-integrated over subsets of the computational domain (traditionally referred to as "nodes") to produce a set of ordinary differential equations, one for each dimension and time for time-dependent problems. These equations then are solved analytically to yield a set of algebraic equations. Approximations are introduced by expanding some of the terms in the differential equation (particularly the nonlinear terms) into series of appropriate functions, which are truncated at the desired order of accuracy.

2.1 The Transverse-Averaged Equations

In Cartesian coordinates, the shallow-water equations become

$$\left.\begin{aligned} &\frac{\partial u}{\partial t} + u\frac{\partial u}{\partial x} + v\frac{\partial u}{\partial y} - fv = K\frac{\partial^2 u}{\partial y^2} + \frac{\partial T_x}{\partial x} \\ &\frac{\partial v}{\partial t} + u\frac{\partial v}{\partial x} + v\frac{\partial v}{\partial y} + fu = K\frac{\partial^2 v}{\partial x^2} + \frac{\partial T_y}{\partial y} \\ &\frac{\partial h}{\partial t} + \frac{\partial F}{\partial x} + \frac{\partial G}{\partial y} = 0 \end{aligned}\right\} \tag{1}$$

where the new quantities that have been introduced are the mass fluxes, defined by $F = hu$ and $G = hv$, and the normal stresses, commonly introduced in the formulation of nodal methods for the Navier-Stokes equations (Azmy, 1983) and defined for the shallow-water equations by

$$T_x = K\frac{\partial u}{\partial x} - \Phi, \qquad T_y = K\frac{\partial v}{\partial y} - \Phi$$

As the first step in the development of the NIM, the nonlinear advective terms, along with certain linear terms, are grouped together, placed on the right-hand sides of

the equations, and incorporated into the definitions of "pseudo-source" terms. The domain then is divided into nodes, each a volume of space-time denoted by $[-a_{i,j},+a_{i,j}]\times[-b_{i,j},+b_{i,j}]\times[0,\Delta t_n]$, and the partial differential equations are transverse averaged locally within each node. Transverse averaging Eq. (1) yields nine ODEs,

$$\left.\begin{array}{lll} \dfrac{d\overline{T}_x^{yt}}{dx}(x)=\overline{S}_1^{yt}(x), & K\dfrac{d^2\overline{u}^{xt}}{dy^2}(y)=\overline{S}_1^{xt}(y), & \dfrac{d\overline{u}^{xy}}{dt}(t)-\overline{f}\overline{v}^{xy}(t)=\overline{S}_1^{xy}(t) \\ K\dfrac{d^2\overline{v}^{yt}}{dx^2}(x)=\overline{S}_2^{yt}(x), & \dfrac{d\overline{T}_y^{xt}}{dy}(y)=\overline{S}_2^{xt}(y), & \dfrac{d\overline{v}^{xy}}{dt}(t)+\overline{f}\overline{u}^{xy}(t)=\overline{S}_2^{xy}(t) \\ \dfrac{d\overline{F}^{yt}}{dx}(x)=\overline{S}_3^{yt}(x), & \dfrac{d\overline{G}^{xt}}{dy}(y)=\overline{S}_3^{xt}(y), & \dfrac{d\overline{h}^{xy}}{dt}(t)=\overline{S}_3^{xy}(t) \end{array}\right\} \quad (2)$$

and transverse averaging the definitions of the normal stresses yields two additional equations,

$$\frac{d\overline{u}^{yt}}{dx}(x)=\overline{S}_4^{yt}(x), \qquad \frac{d\overline{v}^{xt}}{dy}(y)=\overline{S}_4^{xt}(y) \quad (3)$$

where the S quantities are the pseudo-sources, $\overline{f}$ is the average of the Coriolis parameter within the node, and $\overline{p}^{qr}$ denotes the transverse average of a function p in the q- and r-directions, defined by

$$\overline{p}^{qr}(s)=\frac{1}{2q_0}\frac{1}{2r_0}\int_{-r_0}^{+r_0}\int_{-q_0}^{+q_0}p(q,r,s)\,dq\,dr$$

We next solve these equations for the transverse-averaged quantities and evaluate the solutions at the node boundaries to obtain the the discrete-variable equations. Neighboring nodes are coupled by requiring that the transverse-averaged variables and the first derivatives of $\overline{v}^{yt}(x)$ and $\overline{u}^{xt}(y)$ are continuous across node interfaces. Most of the ODEs in Eqs. (2) and (3) can be integrated directly to obtain

$$\overline{T}_x^{yt}(+a_{i,j})-\overline{T}_x^{yt}(-a_{i,j})=\int_{-a_{i,j}}^{+a_{i,j}}\overline{S}_1^{yt}(x')\,dx'$$

and similar equations for $\overline{T}_y^{xt}(y)$, $\overline{F}^{yt}(x)$, $\overline{G}^{xt}(y)$, $\overline{h}^{xy}(t)$, $\overline{u}^{yt}(x)$ and $\overline{v}^{xt}(y)$. The equations for $\overline{v}^{yt}(x)$ and $\overline{u}^{xt}(y)$ must be integrated twice. Eliminating the derivatives of the solutions for $\overline{v}^{yt}(x)$ and $\overline{u}^{xt}(y)$ at the interfaces between adjacent nodes yields

$$\begin{aligned} &K\left[\frac{1}{a_{i+1,j}}\overline{v}^{yt}(+a_{i+1,j})-\left(\frac{1}{a_{i+1,j}}+\frac{1}{a_{i,j}}\right)\overline{v}^{yt}(+a_{i,j})+\frac{1}{a_{i,j}}\overline{v}^{yt}(-a_{i,j})\right] \\ &\quad=\frac{1}{a_{i+1,j}}\int_{-a_{i+1,j}}^{+a_{i+1,j}}\int_{-a_{i+1,j}}^{x'}\overline{S}_2^{yt}(x'')\,dx''\,dx'+\frac{1}{a_{i,j}}\int_{-a_{i,j}}^{+a_{i,j}}\int_{x'}^{+a_{i,j}}\overline{S}_2^{yt}(x'')\,dx''\,dx' \end{aligned}$$

$$K\left[\frac{1}{b_{i,j+1}}\overline{u}^{xt}(+b_{i,j+1})-\left(\frac{1}{b_{i,j+1}}+\frac{1}{b_{i,j}}\right)\overline{y}^{xt}(+b_{i,j})+\frac{1}{b_{i,j}}\overline{u}^{xt}(-b_{i,j})\right]$$
$$=\frac{1}{b_{i,j+1}}\int_{-b_{i,j+1}}^{+b_{i,j+1}}\int_{-b_{i,j+1}}^{y'}\overline{S}_1^{xt}(y'')\,dy''\,dy'+\frac{1}{b_{i,j}}\int_{-b_{i,j}}^{+b_{i,j}}\int_{y'}^{+b_{i,j}}\overline{S}_1^{xt}(y'')\,dy''\,dy'$$

Finally, since the equations for $\overline{u}^{xy}(t)$ and $\overline{v}^{xy}(t)$ are coupled, they must be solved simultaneously, yielding solutions with trigonometric terms

$$\overline{u}^{xy}(t_n)=\overline{u}^{xy}(t_{n-1})\cos\overline{f}\Delta t_n+\overline{v}^{xy}(t_{n-1})\sin\overline{f}\Delta t_n$$
$$+\int_0^{\Delta t_n}\left(\overline{S}_1^{xy}(t_{n-1}+t')\cos\overline{f}(\Delta t_n-t')+\overline{S}_2^{xy}(t_{n-1}+t')\sin\overline{f}(\Delta t_n-t')\right)dt'$$
$$\overline{v}^{xy}(t_n)=\overline{v}^{xy}(t_{n-1})\cos\overline{f}\Delta t_n-\overline{u}^{xy}(t_{n-1})\sin\overline{f}\Delta t_n$$
$$+\int_0^{\Delta t_n}\left(\overline{S}_2^{xy}(t_{n-1}+t')\cos\overline{f}(\Delta t_n-t')-\overline{S}_1^{xy}(t_{n-1}+t')\sin\overline{f}(\Delta t_n-t')\right)dt'$$

2.2 Elimination of the Pseudo-Sources

The discrete equations cannot be solved unless a good estimate of the pseudo-sources is supplied. First, they are approximated within the (i,j)-th node by Legendre expansions that are truncated at first order, leaving only the constant terms. This approximation results in second-order errors in the integrals of the pseudo-sources that appear in the transverse-averaged solutions.

Two additional constraints are used to eliminate the resulting eleven constant pseudo-source terms. The first is the uniqueness of the averages over the (i,j)-th node of the velocity components and geopotential. That is, the nodal average of each quantity $p(q,r,s)$, which is calculated from the transverse average $\overline{p}^{qr}(s)$ by

$$\overline{\overline{p}}^{s}=\frac{1}{2s_0}\int_{-s_0}^{+s_0}\overline{p}^{qr}(s)\,ds$$

must be the same, regardless of the transverse average used in the calculation. Uniqueness of the velocity components averaged over the (i,j)-th node yields four equations:

$$\overline{\overline{u}}^{x}_{i,j}=\overline{\overline{u}}^{y}_{i,j}=\overline{\overline{u}}^{t}_{i,j}$$
$$\overline{\overline{v}}^{x}_{i,j}=\overline{\overline{v}}^{y}_{i,j}=\overline{\overline{v}}^{t}_{i,j}$$

To provide the second constraint, the original PDEs in Eq. (1), the definitions of the normal stresses, and the definitions of the mass fluxes are averaged over each node, and the resulting equations are evaluated in terms of the transverse-averaged quantities on the node interfaces (which are the discrete-variable unknowns) and the constant pseudo-sources terms. Averaging Eq. (1) ensures that momentum and mass are conserved over

each node and results in

$$\left.\begin{aligned}
&\overline{S}^{yt}_{1,i,j}+\overline{S}^{xt}_{1,i,j}-\overline{S}^{xy}_{1,i,j}+\beta\left[\overline{y\overline{v}^{xt}}^{y}\right]_{i,j}\\
&\qquad=\frac{1}{4a_{i,j}b_{i,j}\Delta t_n}\int_{t_{n-1}}^{t_n}\int_{-b_{i,j}}^{+b_{i,j}}\int_{-a_{i,j}}^{+a_{i,j}}\left(u\frac{\partial u}{\partial x}+v\frac{\partial u}{\partial y}\right)dx\,dy\,dt\\
&\overline{S}^{yt}_{2,i,j}+\overline{S}^{xt}_{2,i,j}-\overline{S}^{xy}_{2,i,j}-\beta\left[\overline{y\overline{u}^{xt}}^{y}\right]_{i,j}\\
&\qquad=\frac{1}{4a_{i,j}b_{i,j}\Delta t_n}\int_{t_{n-1}}^{t_n}\int_{-b_{i,j}}^{+b_{i,j}}\int_{-a_{i,j}}^{+a_{i,j}}\left(u\frac{\partial v}{\partial x}+v\frac{\partial v}{\partial y}\right)dx\,dy\,dt\\
&\overline{S}^{yt}_{3,i,j}+\overline{S}^{xt}_{3,i,j}+\overline{S}^{xy}_{3,i,j}=0
\end{aligned}\right\}\qquad(4)$$

Averaging the definitions of the normal stresses and fluxes provides the remaining four equations needed to solve for the pseudo-source terms:

$$\begin{aligned}
\overline{S}^{yt}_{4,i,j}&=\overline{\overline{T}}^{x}_{x,i,j}+\overline{\overline{\Phi}}^{t}_{i,j}, &\qquad \overline{S}^{xt}_{4,i,j}&=\overline{\overline{T}}^{y}_{y,i,j}+\overline{\overline{\Phi}}^{t}_{i,j}\\
\overline{\overline{F}}^{x}_{i,j}&=[\overline{\overline{uh}}]_{i,j}, &\qquad \overline{\overline{G}}^{y}_{i,j}&=[\overline{\overline{vh}}]_{i,j}
\end{aligned}$$

Since the last two equations involve averages of products, $\overline{\overline{uh}}$ and $\overline{\overline{vh}}$, and since the advective terms on the RHS of Eqs. (4) are not readily evaluated in terms of known quantities, these products must be approximated. This is accomplished by Legendre expanding each term in the product and truncating the expansions at first order, which results in a second-order error in the average. (This procedure is equivalent to replacing the average of each product $\overline{pq}$ by the product of the averages of the individual factors $\overline{p}\,\overline{q}$.)

2.3 The Discrete-Variable Equations

The additional constraints introduced in the preceding subsection are sufficient to express the pseudo-sources in terms of the discrete-variable unknowns. Furthermore, by coupling the transverse-averaged equations for the normal stresses in neighboring nodes, $\overline{T}^{yt}_{x}$ can be eliminated at the interfaces between nodes in the x-direction, leaving $\overline{u}^{yt}$, $\overline{v}^{yt}$ and $\overline{F}^{yt}$ as the only yt-averaged unknowns, and $\overline{T}^{xt}_{y}$ can be eliminated at the interfaces between nodes in the y-direction, leaving $\overline{u}^{xt}$, $\overline{v}^{xt}$ and $\overline{G}^{xt}$ as the only xt-averaged unknowns. Finally, the fluid depth h can be replaced everywhere by the geopotential Φ by introducing the average height of the rigid bottom $\overline{h}_{\mathrm{B}}$ within each node.

After eliminating all the pseudo-sources except $\overline{S}^{yt}_{1}$ and $\overline{S}^{xt}_{2}$ from the equations, we obtain

$$\begin{aligned}
&K\left[\frac{1}{a_{i+1,j}}\overline{u}^{yt}(+a_{i+1,j})-\left(\frac{1}{a_{i+1,j}}+\frac{1}{a_{i,j}}\right)\overline{u}^{yt}(+a_{i,j})+\frac{1}{a_{i,j}}\overline{u}^{yt}(-a_{i,j})\right]\\
&\qquad+\overline{\Phi}^{xy}_{i}(t_n)-\overline{\Phi}^{xy}_{i+1}(t_n)+\overline{\Phi}^{xy}_{i}(t_{n-1})-\overline{\Phi}^{xy}_{i+1}(t_{n-1})=2a_{i,j}\overline{S}^{yt}_{1,i,j}+2a_{i+1,j}\overline{S}^{yt}_{1,i+1,j}
\end{aligned}$$

$$\frac{1}{a_{i+1,j}}\overline{v}^{yt}(+a_{i+1,j})+\left(\frac{2}{a_{i+1,j}}+\frac{2}{a_{i,j}}\right)\overline{v}^{yt}(+a_{i,j})+\frac{1}{a_{i,j}}\overline{v}^{yt}(-a_{i,j})$$
$$=3\left(\frac{\overline{v}^{xt}(+b_{i,j})+\overline{v}^{xt}(-b_{i,j})}{2a_{i,j}}+\frac{\overline{v}^{xt}(+b_{i+1,j})+\overline{v}^{xt}(-b_{i+1,j})}{2a_{i+1,j}}\right)$$

$$\left(\overline{u}^{yt}(+a_{i,j})+\overline{u}^{yt}(-a_{i,j})\right)\left(\frac{\overline{\Phi}^{xy}(t_n)+\overline{\Phi}^{xy}(t_{n-1})}{2g}-\overline{h}_{\mathrm{B}}\right)=\overline{F}^{yt}(+a_{i,j})+\overline{F}^{yt}(-a_{i,j})$$

$$\frac{1}{b_{i,j+1}}\overline{u}^{xt}(+b_{i,j+1})+\left(\frac{2}{b_{i,j+1}}+\frac{2}{b_{i,j}}\right)\overline{u}^{xt}(+b_{i,j})+\frac{1}{b_{i,j}}\overline{u}^{xt}(-b_{i,j})$$
$$=3\left(\frac{\overline{u}^{yt}(+a_{i,j})+\overline{u}^{yt}(-a_{i,j})}{2b_{i,j}}+\frac{\overline{u}^{yt}(+a_{i,j+1})+\overline{u}^{yt}(-a_{i,j+1})}{2b_{i,j+1}}\right)$$

$$K\left[\frac{1}{b_{i,j+1}}\overline{v}^{xt}(+b_{i,j+1})-\left(\frac{1}{b_{i,j+1}}+\frac{1}{b_{i,j}}\right)\overline{v}^{xt}(+b_{i,j})+\frac{1}{b_{i,j}}\overline{v}^{xt}(-b_{i,j})\right]$$
$$+\overline{\Phi}^{xy}_{j}(t_n)-\overline{\Phi}^{xy}_{j+1}(t_n)+\overline{\Phi}^{xy}_{j}(t_{n-1})-\overline{\Phi}^{xy}_{j+1}(t_{n-1})=2b_{i,j}\overline{S}^{xt}_{2,i,j}+2b_{i,j+1}\overline{S}^{xt}_{2,i,j+1}$$

$$\left(\overline{v}^{xt}(+b_{i,j})+\overline{v}^{xt}(-b_{i,j})\right)\left(\frac{\overline{\Phi}^{xy}(t_n)+\overline{\Phi}^{xy}(t_{n-1})}{2g}-\overline{h}_{\mathrm{B}}\right)=\overline{G}^{xt}(+b_{i,j})+\overline{G}^{xt}(-b_{i,j})$$

$$\overline{u}^{xy}(t_n)=C_{1,n}\left(\overline{u}^{yt}(+a_{i,j})+\overline{u}^{yt}(-a_{i,j})\right)+C_{2,n}\overline{u}^{xy}(t_{n-1})$$
$$-C_{3,n}\left[\tfrac{1}{2}\left(\overline{v}^{xt}(+b_{i,j})+\overline{v}^{xt}(-b_{i,j})\right)-\overline{v}^{xy}(t_{n-1})\right]$$

$$\overline{v}^{xy}(t_n)=C_{1,n}\left(\overline{v}^{xt}(+b_{i,j})+\overline{v}^{xt}(-b_{i,j})\right)+C_{2,n}\overline{v}^{xy}(t_{n-1})$$
$$+C_{3,n}\left[\tfrac{1}{2}\left(\overline{u}^{yt}(+a_{i,j})+\overline{u}^{yt}(-a_{i,j})\right)-\overline{u}^{xy}(t_{n-1})\right]$$

$$\overline{\Phi}^{xy}(t_n)=\overline{\Phi}^{xy}(t_{n-1})-\Delta t_n\, g\left(\frac{\overline{F}^{yt}(+a_{i,j})-\overline{F}^{yt}(-a_{i,j})}{2a_{i,j}}+\frac{\overline{G}^{xt}(+b_{i,j})-\overline{G}^{xt}(-b_{i,j})}{2b_{i,j}}\right)$$

where all the time-averaged unknowns (e.g., $\overline{u}^{yt}(+a_{i,j})$ and $\overline{v}^{xt}(+b_{i,j})$) are averaged over the n-th time step and the subscript n is suppressed. The remaining pseudo-sources are given by

$$\overline{S}^{yt}_{1,i,j}=\tfrac{1}{2}\overline{f}\cot(\overline{f}\Delta t_n/2)\left(\overline{u}^{xy}(t_n)-\overline{u}^{xy}(t_{n-1})\right)-\tfrac{1}{2}\overline{f}\left(\overline{v}^{xy}(t_n)+\overline{v}^{xy}(t_{n-1})\right)$$
$$+3K\frac{\overline{u}^{yt}(+a_{i,j})+\overline{u}^{yt}(-a_{i,j})-\overline{u}^{xt}(+b_{i,j})-\overline{u}^{xt}(-b_{i,j})}{2b^2_{i,j}}$$
$$-\beta b_{i,j}\frac{\overline{v}^{xt}(+b_{i,j})-\overline{v}^{xt}(-b_{i,j})}{6}+\frac{\left[\overline{u}^{yt}(+a_{i,j})\right]^2-\left[\overline{u}^{yt}(-a_{i,j})\right]^2}{4a_{i,j}}$$
$$+\frac{\left(\overline{v}^{xt}(+b_{i,j})+\overline{v}^{xt}(-b_{i,j})\right)\left(\overline{u}^{xt}(+b_{i,j})-\overline{u}^{xt}(-b_{i,j})\right)}{4b_{i,j}}$$

$$\overline{S}^{xt}_{2,i,j} = \tfrac{1}{2}\bar{f}\cot(\bar{f}\Delta t_n/2)\left(\bar{v}^{xy}(t_n)-\bar{v}^{xy}(t_{n-1})\right)+\tfrac{1}{2}\bar{f}\left(\bar{u}^{xy}(t_n)+\bar{u}^{xy}(t_{n-1})\right)$$
$$+3K\frac{\bar{v}^{xt}(+b_{i,j})+\bar{v}^{xt}(-b_{i,j})-\bar{v}^{yt}(+a_{i,j})-\bar{v}^{yt}(-a_{i,j})}{2a^2_{i,j}}$$
$$+\beta b_{i,j}\frac{\bar{u}^{xt}(+b_{i,j})-\bar{u}^{xt}(-b_{i,j})}{6}+\frac{\left[\bar{v}^{xt}(+b_{i,j})\right]^2-\left[\bar{v}^{xt}(-b_{i,j})\right]^2}{4b_{i,j}}$$
$$+\frac{\left(\bar{u}^{yt}(+a_{i,j})+\bar{u}^{yt}(-a_{i,j})\right)\left(\bar{v}^{yt}(+a_{i,j})-\bar{v}^{yt}(-a_{i,j})\right)}{4a_{i,j}}$$

and the trigonometric terms that appear in the solutions for $\bar{u}^{xy}$ and $\bar{v}^{xy}$ have been incorporated into the coefficients $C_{1,n}$, $C_{2,n}$ and $C_{3,n}$, defined as

$$C_{1,n}=\frac{\frac{1}{4}\bar{f}^2\Delta t_n^2\left[1-\cos(\bar{f}\Delta t_n)\right]}{1+\frac{1}{2}\bar{f}^2\Delta t_n^2-\cos(\bar{f}\Delta t_n)-\bar{f}\Delta t_n\sin(\bar{f}\Delta t_n)}$$

$$C_{2,n}=\frac{1+(\frac{1}{2}\bar{f}^2\Delta t_n^2-1)\cos(\bar{f}\Delta t_n)-\bar{f}\Delta t_n\sin(\bar{f}\Delta t_n)}{1+\frac{1}{2}\bar{f}^2\Delta t_n^2-\cos(\bar{f}\Delta t_n)-\bar{f}\Delta t_n\sin(\bar{f}\Delta t_n)}$$

$$C_{3,n}=\frac{\bar{f}\Delta t_n\left[\cos(\bar{f}\Delta t_n)-1+\frac{1}{2}\bar{f}\Delta t_n\sin(\bar{f}\Delta t_n)\right]}{1+\frac{1}{2}\bar{f}^2\Delta t_n^2-\cos(\bar{f}\Delta t_n)-\bar{f}\Delta t_n\sin(\bar{f}\Delta t_n)}$$

This is the final set of discrete-variable equations for the NIM, expressed in terms of the transverse-averaged velocity components and normal fluxes along the spatial interfaces of the nodes and the transverse-averaged velocity components and geopotential at the end of each time step. When combined with an appropriate set of boundary conditions, this set of equations forms a nonlinear algebraic problem, which we solve for each time step using a Newton-Krylov method (Brown, 1990).

3. NUMERICAL RESULTS

The new NIM was applied to the numerical solution of several shallow-water problems in Cartesian geometries. First, it was tested using two simple steady-state problems with known analytical solutions. Next, it was tested using a modified system, which allowed the formation and propagation of atmospheric disturbances with known analytical solutions. Finally, the method was used to solve two problems of special interest: flow over mountains and flow induced by a jet.

The two steady-state problems were solved on a $4,000\,\text{km}\times 4,000\,\text{km}$ domain, subdivided by a 16×16 mesh, with a constant Coriolis parameter (i.e., $\beta=0$). The solution for the first problem has a uniform velocity field and a linearly sloping upper surface; that for the second problem has a uniform vorticity field (rotating flow) and parabolic upper surface. For each test problem, the analytical steady-state solution was supplied as a boundary condition along the edge of the mesh—the velocity components along the entire boundary and the normal mass fluxes on the upstream boundaries only. Starting from rather general

initial conditions, the (time-dependent) solver converged to the asymptotic (steady-state) solution through the action of the boundary conditions and the dissipative term (with coefficient $K = 10^7\,\mathrm{m}^2/\mathrm{s}$). After 360 hours of simulated time (120 time steps of 3 hours each), the relative differences between the computed solutions and the analytical solutions, due to both the numerical error and the fact that the finite time numerical solutions are not truly time-asymptotic solutions, were 0.9056 and 0.7005 percent for the constant velocity and constant vorticity problems, respectively. In these results, the relative "difference" is defined as the L_1 norm of the difference divided by the L_1 norm of the unknown quantities—the velocity components, mass fluxes and geopotential, all scaled to order unity. Assuming that there is not a fortuitous cancellation between the numerical error and the difference between the numerical solution at 360 hours and time-asymptotic numerical solution, this indicates that the new NIM for the shallow-water equations yields accurate solutions even on a coarse 16×16 mesh.

The remaining problems were set in a β-plane channel. This system is periodic in the *x*-direction (east-west) with frictionless, rigid boundaries along the north and south edges, which allow no normal flow ($v = 0$) and no shear stress ($\partial u/\partial y = 0$). Although no nontrivial closed-form solutions for this problem are known, the problem can be modified slightly, by imposing a rigid lid on the upper surface, thereby forcing the flow to be nondivergent and allowing analytical solutions to be obtained. These analytical solutions take the form of Rossby waves, large-scale disturbances of meteorological interest, which owe their existence to the variation of the Coriolis parameter with latitude.

The Rossby wave solutions to the shallow-water model with a rigid lid were used to create a test problem for the shallow-water model with a free upper surface. This was done by adding source terms to the equations of motion, so that the modified version of these equations has the Rossby wave as an exact analytical solution, and the NIM was applied to the resulting test problem. Two source terms were used. The first was added to the mass equation to force the flow to be nondivergent; the second was added to the momentum equations to cancel the effects of the dissipative term (otherwise, the Rossby wave would quickly decay to uniform east-west flow).

When a Rossby wave solution was supplied as the initial condition, the NIM was able to propagate the wave indefinitely, exceeding ten years of simulated time with little deterioration. The results of one such calculation, for a $7,500\,\mathrm{km} \times 4,000\,\mathrm{km}$ domain, done on a 15×8 mesh with an 8 hour time step, $K = 5 \times 10^5\,\mathrm{m}^2/\mathrm{s}$ and the initial condition in Fig. 1, is shown in Fig. 2 after 12 years of simulated time. When compared to the analytical solution, this solution had a relative error of 14.54 percent after 100 days of simulated time.

Free propagating Rossby modes normally are only weakly excited in the atmosphere. Other, stronger Rossby modes, which are of great importance in determining planetary circulation patterns, are produced in the atmosphere by flow over topography. Therefore, in the next series of tests, the height of the rigid bottom h_B was altered to produce such forced stationary topographic Rossby waves.

An obstacle, representing a mountain with a height approximately a third of the

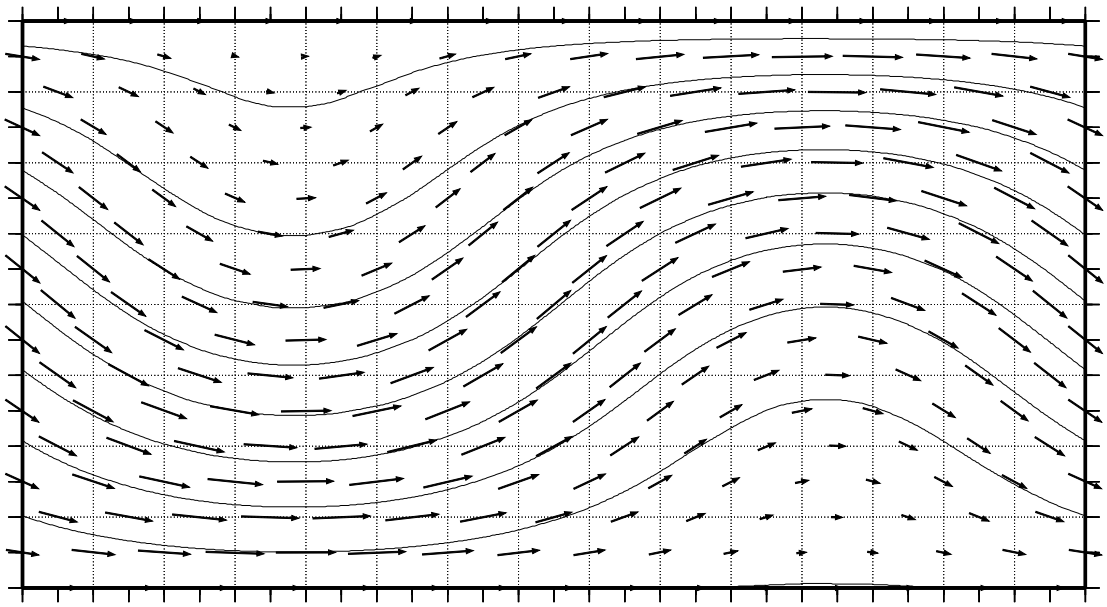

Fig. 1 The velocity field (arrows) and geopotential (contours) of the Rossby wave with a background wind speed of 4.7 m/s supplied on a $7,500\,\text{km} \times 4,000\,\text{km}$ domain and a 15×8 mesh as the initial condition to the modified "rigid lid" test problem.

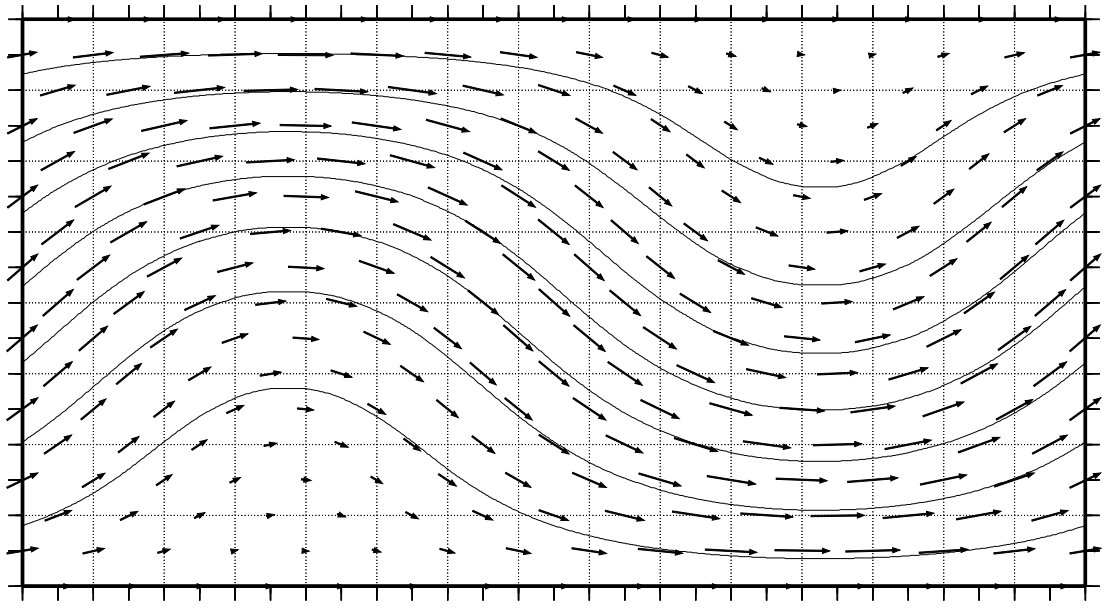

Fig. 2 The velocity field (arrows) and geopotential (contours) of the freely-propagating Rossby wave solution to the modified "rigid lid" problem with a background wind speed of 4.7 m/s, calculated for a $7,500\,\text{km} \times 4,000\,\text{km}$ domain after 12 years of simulated time via the new NIM with $K = 5 \times 10^5\,\text{m}^2/\text{s}$, an 8 hour time step and a 15×8 mesh.

average free-surface height, was placed in the path of a uniform flow in the x-direction. The topographical Rossby wave generated by this obstacle is shown, as computed on a 15×8 mesh, in Fig. 3. This calculation was repeated on other meshes, and the results compared. Those from a 31×15 mesh calculation, shown in Fig. 4, are very similar to the coarse mesh results, shown in Fig. 3, indicating that the method yields accurate results on coarse meshes.

Finally, the effect of the dissipative term was studied by imposing a forced flow (or jet) on the vertical interface between two nodes. Several combinations of jet and background wind velocities were studied, including flow in which the jet was imposed on a motionless fluid, as shown in Fig. 5, and flow in which the jet was directed counter to the background wind, as shown in Fig. 6. Once again, the fine mesh calculations were compared to coarser mesh calculations, and the agreement between the two confirmed the ability of the method to yield accurate results on coarse meshes.

4. CONCLUSIONS

We have developed a new nodal integral method for the shallow-water equations with Coriolis force and a second-order, linear dissipative term. The formalism is similar to, but more complicated than, those of other nodal methods for fluid flow problems. Applications to simple test problems and fairly complicated Rossby wave problems with analytical solutions have established its computational stability and accuracy. Other tests, using complex benchmark problems involving flows over obstacles and jet-driven flows, have demonstrated the ability of the new method to model important horizontal flow aspects of atmospheric dynamics.

ACKNOWLEDGEMENT

This research was supported by the U.S. National Aeronautics and Space Administration under Grant No. NAG5-3973.

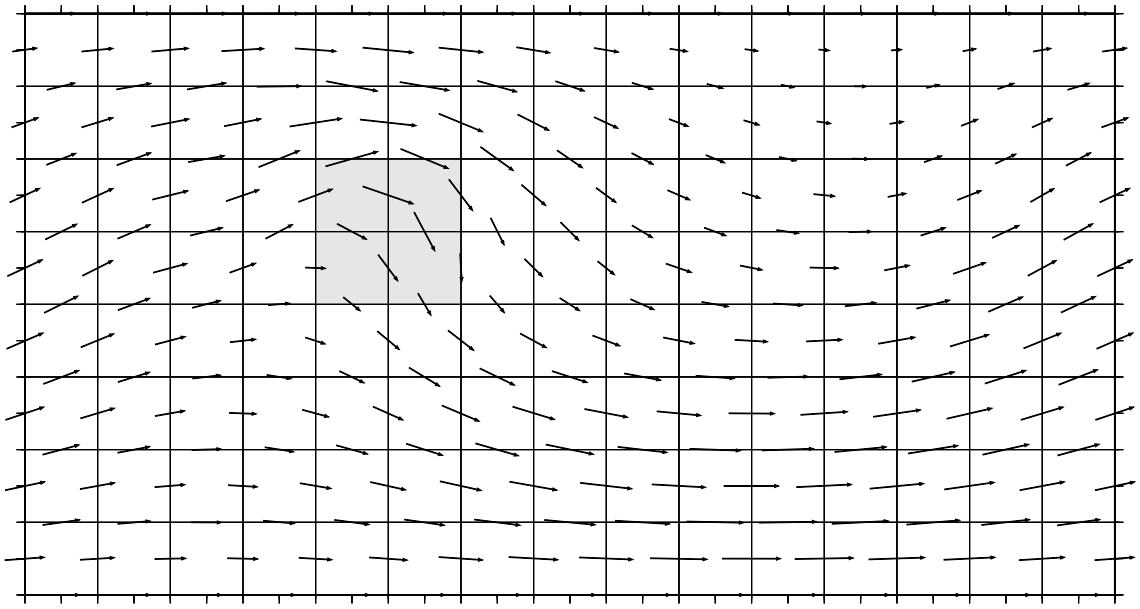

Fig. 3 The velocity field of a stationary topographical Rossby wave in a $7,500\,\text{km} \times 4,000\,\text{km}$ domain generated by flow over a $1,000\,\text{km} \times 1,000\,\text{km} \times 2\,\text{km}$ obstacle after 90 hours of simulation time calculated via the new NIM on a 15×8 mesh using a 3 hour time step. Average background wind speed was $20\,\text{m/s}$, average height of the free surface was 5.60 km (at 90 hours), and K was $10^6\,\text{m}^2/\text{s}$

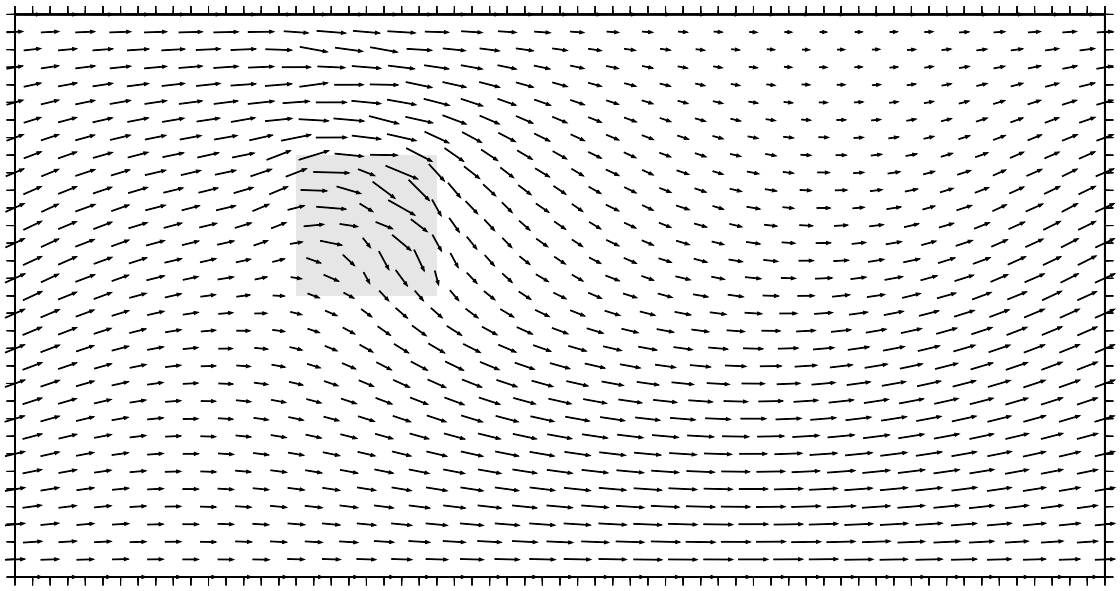

Fig. 4 The velocity field of a stationary topographical Rossby wave in a $7,750\,\text{km} \times 4,000\,\text{km}$ domain generated by flow over a $1,000\,\text{km} \times 1,000\,\text{km} \times 2\,\text{km}$ obstacle after 90 hours of simulation time calculated via the new NIM on a 31×15 mesh using a 3 hour time step. Average background wind speed was $20\,\text{m/s}$, average height of the free surface was 5.57 km (at 90 hours), and K was $10^6\,\text{m}^2/\text{s}$

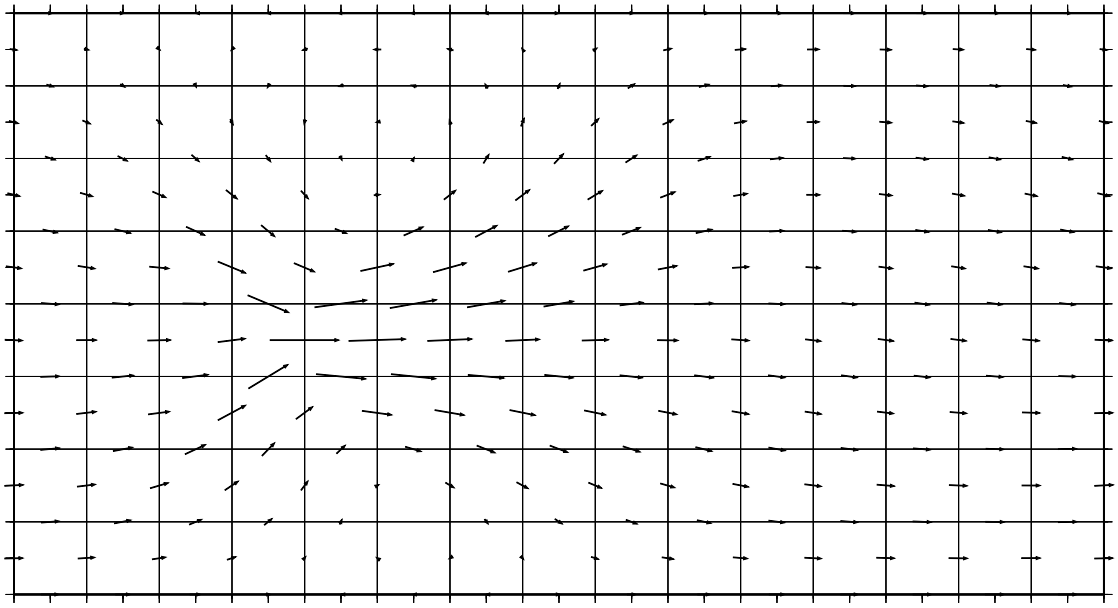

Fig. 5 The velocity field in a $7,500\,\mathrm{km} \times 4,000\,\mathrm{km}$ domain, induced by a 500 km wide jet, after 90 hours of simulation time calculated via the new NIM on a 15×8 mesh using a 3 hour time step. The jet speed was $20\,\mathrm{m/s}$, the average background wind speed was $10\,\mathrm{m/s}$, and K was $2 \times 10^6\,\mathrm{m^2/s}$. The jet was imposed on the right surface of the 4-4 (x-y) node measured from the lower left corner of the domain.

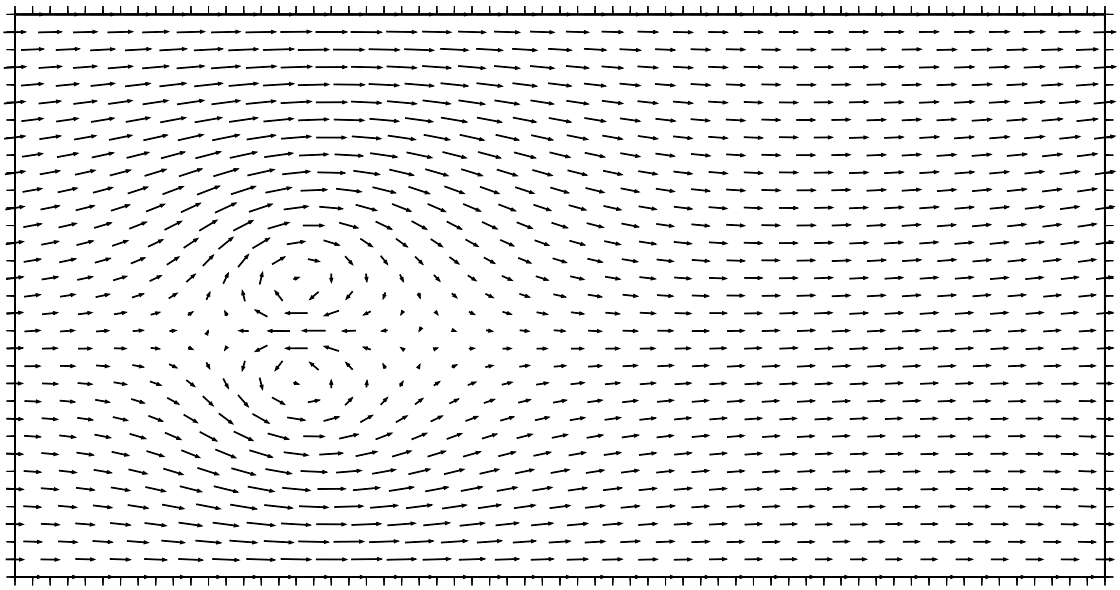

Fig. 6 The velocity field in a $7,750\,\mathrm{km} \times 4,000\,\mathrm{km}$ domain, induced by a 500 km wide counter-flowing jet, after 90 hours of simulation time calculated via the new NIM on a 31×16 mesh using a 3 hour time step. The counter-flowing jet speed and average background wind speed were both $10\,\mathrm{m/s}$, and K was $2 \times 10^6\,\mathrm{m^2/s}$. The jet was imposed on the right surfaces of the 8-7 and 8-8 (x-y) nodes measured from the lower left corner of the domain.

REFERENCES

Azmy, Y.Y., Dorning, J.J., 1983. A nodal integral approach to the numerical solution of partial differential equations. In: *Advances in Reactor Computations*, Vol. II, American Nuclear Society, LaGrange Park, IL, pp. 893–909.

Azmy, Y.Y., Dorning, J.J., 1984. Arc-length continuation of nodal integral method solutions to the nonlinear Navier-Stokes equations. In: Taylor, C., Hinton, E., Owen, D.R.J., Oñate, E. (Eds.), *Numerical Methods for Nonlinear Problems II*, Pineridge Press, Swansea, U. K., pp. 672–687.

Azmy, Y.Y., Dorning, J.J., 1986. Numerical studies of bifurcations in the confined Bénard problem. In: Zhuang, F.G., Zhu, Y.L. (Eds.), *Proc. Tenth Int. Conf. Numerical Methods in Fluid Dynamics*, Springer-Verlag, Berlin, pp. 96–104.

Brown, P.N., Saad, Y., 1990. Hybrid Krylov methods for nonlinear systems of equations. *SIAM J. Sci. Stat. Comp.* **11**, 450–481.

Decker, W.J., Dorning, J.J., 1993. A block iterative nodal integral method for fluid dynamics problems. In: *Mathematical Methods and Supercomputing in Nuclear Applications*, Kernforschungszentrum Karlsruhe GmbH, Karlsruhe, Germany, pp. 208–223.

Hannon, J.P., Holloway, J.P., Dorning, J.J., 1991. A nodal method for the inviscid shallow-water equations. In: *Advances in Mathematics, Computations, and Reactor Physics*, University Graphics and Printing, University of Pittsburg, Pittsburgh, PA, pp. 6.2 2–1 – 6.2 2–13.

Horak, W.C., Dorning, J.J., 1985. A nodal coarse-mesh method for the efficient numerical solution of laminar flow problems. *J. Comp. Phys.* **59**, 405–440.

Wilson, G.L., Rydin, R.A., Azmy, Y.Y., 1987. Time-dependent nodal integral methods in fluid dynamics. In: *Advances in Reactor Physics, Mathematics, and Computation*, Section Francaise de L'American Nuclear Society, Paris, France, pp. 1681–1695.